

Theory of two-phonon modes in layered charge-density-wave systems

S N BEHERA and G C MOHANTY

Institute of Physics, Bhubaneswar 751 005, India

MS received 24 May 1985

Abstract. A theoretical model with electron-phonon and anharmonic interactions is proposed to explain the two-phonon mode observed in the Raman spectra of layered transition metal dichalcogenides, which exhibit charge density wave (CDW) phase transition. The phonon self-energy, which involves the electron response function and the two-phonon Green's function, is calculated using the double-time Green's function formalism. It is shown that in these low-dimensional systems there exists an anharmonicity-mediated two-phonon mode in the phonon spectral function both in the normal and in the CDW phases. In the normal phase since the phonon Raman scattering proceeds through a single optic phonon the calculations are carried out for zero wave vector and hence the contribution of the electron response function to the self-energy vanishes. On the other hand explicit evaluation of the two-phonon Green's function shows that the frequency of the two-phonon mode is twice that of the Kohn anomaly phonon and decreases with decreasing temperature. The strength of the two-phonon peak is found to be comparable to that of the original optic phonon. In the CDW phase the phonon which enters into the Raman scattering is taken to be the one with the CDW wave vector Q , which when zone-folded becomes equivalent to zero wave vector. The evaluation of the electron response function in this phase generates a phonon corresponding to the CDW-amplitude mode. The two-phonon Green's function is assumed to be of similar form as in the normal phase. The spectral function evaluated at zero temperature shows a weak two-phonon peak besides the prominent CDW-amplitude mode. Numerical results are presented for the system $2H-NbSe_2$ and are found to be in qualitative agreement with the experimental data.

Keywords. Two-phonon modes; layered compounds; Raman scattering; charge density waves; anharmonicity; electron-phonon interaction; Kohn anomaly.

PACS No. 63-20; 78-30

1. Introduction

In certain transition metal compounds strong two-phonon modes have been observed (Klein 1982a) by Raman scattering. Among these are one class of compounds like the transition metal carbides (Wipf *et al* 1981) and nitrides (Spengler and Kaiser 1976) which have rock-salt structure. However, the compounds showing most spectacular two-phonon modes are the transition metal dichalcogenides, which have layered structure, exist as different polytypes, and exhibit charge density wave (CDW) phase transitions (Wilson *et al* 1975). We briefly summarize some of the properties (pertinent to the observed two-phonon mode) of these transition metal dichalcogenides. The 1T polytypes of these compounds do not exist in the normal phase whereas the 2H-polytypes are found in the normal phase at room temperature and undergo CDW transitions at lower temperatures. The transition temperatures for $2H-NbSe_2$ and $TaSe_2$ are respectively 33 K and 120 K. In these systems the phase transition is driven

by the partial softening (Kohn anomaly) of LA phonons near a wave vector $q = (2/3)\Gamma M$ in the basal plane of the hexagonal Brillouin zone. From the neutron scattering measurements of Moncton *et al* (1977) the frequencies of the Kohn anomaly phonon for 2H-TaSe₂ are known to be 58 cm⁻¹ at 300 K and 37 cm⁻¹ at 122 K. In the normal phase, the most intense feature in the 300 K Raman spectra of 2H-NbSe₂ (Tsang *et al* 1976; Sooryakumar *et al* 1981) is the broad two-phonon peak at 180 cm⁻¹ in A_{1g} spectrum and 175 cm⁻¹ in the E_{2g} spectrum. These peaks soften to 160 and 150 cm⁻¹ respectively at 100 K. Similar two-phonon Raman peaks are also observed in 2H-TaSe₂ (Smith *et al* 1976; Steigmeier *et al* 1976; Sugai and Murase 1982) near 135 cm⁻¹ at room temperature which softens as temperature decreases. The frequencies of these two-phonon peaks are found to be approximately twice those of the Kohn anomaly phonons and show strong softening with decreasing temperature. This is a prelude to the CDW phase transition. The measurements show that the two-phonon peaks also persist below the CDW transition. However in this phase the frequency hardens (Sugai and Murase 1982) with decreasing temperature.

The first attempt to provide a theoretical explanation of the two-phonon Raman mode was due to Maladague and Tsang (1978). They considered the contribution of the phonon-assisted electronic light scattering process to the two-phonon Raman amplitude, and succeeded in demonstrating that the matrix element of the scattering process is proportional to the electronic polarizability. Normally the two-phonon Raman scattering, being a higher order process, the associated intensities are expected to be weak. However for low-dimensional systems the electronic-polarizability develops a singularity at the wave-vector $2k_F$ which in turn results in the enhancement of the intensity of the two-phonon Raman line (the two-phonons having wave vectors $+2k_F$ and $-2k_F$ respectively). Since the same singularity also enters into the phonon self-energy giving rise to the Kohn anomaly, the enhancement of the two-phonon Raman amplitude will depend on the magnitude of the Kohn anomaly. Klein (1981) has generalized these ideas and given a formal derivation of the Raman scattering amplitude using Kawabata's (1971) Green's function formalism, in which the two-phonon contribution comes from the evaluation of the four-vertex function to second order. Recently Nagaosa and Hanamura (1984) have given detailed description of Raman and infrared spectra of transition metal dichalcogenides in the CDW state in terms of hybridization and multiphonon processes in which condensed phonons participate. They also use the Maladague-Tsang mechanism for two-phonon modes.

In the present paper we provide an alternative explanation of the two-phonon modes observed in the layered compounds. It is well known that in low-dimensional conductors strong electron-phonon interaction is responsible for the pronounced Kohn anomaly and subsequent CDW formation. The CDW state is always accompanied by a distortion of the lattice (Friend and Jerome 1979; Klein 1982a) which indicates that these systems are highly anharmonic. The importance of anharmonicity in these systems (the layered compounds in particular) in the context of Raman scattering has been emphasized by Nagaosa and Hanamura (1982, 1984) and Klein (1982b). These authors invoke the presence of a cubic anharmonic term in order to explain the observed CDW amplitude and phase modes in these compounds. Rietschel (1974) also showed that for one-dimensional systems cubic and quartic anharmonicities exhibit pronounced resonance structure around the q -point where Kohn anomaly occurs. In these materials the Raman scattering mechanism can be described as follows: an incident photon excites an electron-hole pair which in turn can couple to an optic phonon through

electron-phonon interaction. This phonon might decay to two-phonons of equal and opposite wave vectors via cubic anharmonicity giving rise to a two-phonon peak in the phonon spectral function (Behera and Samsur 1981). This two-phonon peak can carry the signature of the Kohn-anomaly phonon if the two wave-vectors are $\pm 2k_F$, and can be seen by light scattering. Moreover, since the scattering proceeds through a one-phonon process, the relative intensity in this case is expected to be higher than in a two-phonon process. Hence we consider a model system with electron-phonon and anharmonic interactions and calculate the phonon self-energy using the double time Green's function technique (Zubarev 1960). We show that in these low-dimensional systems an anharmonicity-mediated two-phonon peak exists both above and below the CDW transition and exhibits the characteristic energy and temperature dependence of the observed Raman mode.

The problem is formulated in §2 and the phonon self-energy is evaluated for (i) the normal and (ii) the CDW phases. Section 3 is devoted to the analysis of the phonon spectral function for the above two cases. We conclude in §4 with a discussion of the relevance of our results to the Raman scattering observations in layered compounds.

2. Theory

We consider a model system with the Hamiltonian

$$H = H_e + H_p + H_{e-p} + H_a, \quad (1a)$$

where

$$H_e = \sum_{k\sigma} \varepsilon_k C_{k\sigma}^\dagger C_{k\sigma} \quad (1b)$$

describes free electrons, $C_{k\sigma}$ ($C_{k\sigma}^\dagger$) being the annihilation (creation) operator for an electron with momentum k and spin σ having energy ε_k ,

$$H_p = \sum_q \omega_q b_q^\dagger b_q \quad (1c)$$

is the free phonon Hamiltonian, b_q (b_q^\dagger) being the corresponding operators for phonons with wave vector q and frequency ω_q ,

$$H_{e-p} = g \sum_{qk\sigma} C_{k+q\sigma}^\dagger C_{k\sigma} A_q \quad (1d)$$

denotes the electron-phonon-interaction with coupling constant g ,

$$H_a = \alpha \sum_{q_1 q_2 q_3} A_{q_1} A_{q_2} A_{q_3} \quad (1e)$$

describes the cubic anharmonic interaction, whose strength is given by the parameter α , and

$$A_q = b_q + b_{-q}^\dagger \quad B_q = b_q - b_{-q}^\dagger \quad (1f)$$

are respectively the q th Fourier components of the displacement and momentum of phonons. We shall implicitly assume the presence of a quartic anharmonic term as well

in (1e) for stability considerations, but ignore it in the rest of the calculations keeping in mind the fact that in the lowest order approximation the quartic term modifies the harmonic frequency ω_q providing a temperature-dependence to it.

Since we are interested in the phonon Raman scattering in layered compounds, we calculate the phonon Green's function which is defined as (Zubarev 1960)

$$\begin{aligned} D_{qq'}(t-t') &\equiv \langle\langle A_q(t); A_{q'}^\dagger(t') \rangle\rangle \\ &= -i\theta(t-t') \langle [A_q(t), A_{q'}^\dagger(t')] \rangle. \end{aligned} \quad (2)$$

The Fourier-transformed equation of motion for $D_{qq'}$ evaluated for the system defined by Hamiltonian (1) becomes

$$D_{qq'}(\omega) = \delta_{qq'}(\omega_q/\pi)[\omega^2 - \omega_q^2 - \Sigma_q(\omega)]^{-1}, \quad (3)$$

the phonon self-energy $\Sigma_q(\omega)$ being

$$\begin{aligned} \Sigma_q(\omega) &= 4\pi\omega_q[(3\alpha/\pi)\sum_q \langle A_q \rangle + g^2\chi_q(\omega) + q\alpha^2\Gamma_q(\omega) \\ &\quad + 3g\alpha(\Gamma'_q(\omega) + \Gamma''_q(\omega))], \end{aligned} \quad (4)$$

where $\langle A_q \rangle$ is the thermal average of the displacement operator A_q ,

$$\chi_q(\omega) = \sum_{k\sigma, k'\sigma'} \langle\langle C_{k-q\sigma}^\dagger(t)C_{k\sigma}(t); C_{k'+q\sigma'}^\dagger(t')C_{k'\sigma'}(t') \rangle\rangle_\omega \quad (5)$$

is the electron response function,

$$\Gamma_q(\omega) = \sum_{q_1 \dots q_n} \langle\langle A_{q_1}(t)A_{q_2}(t); A_{q_3}(t')A_{q_n}(t') \rangle\rangle_\omega \quad (6)$$

is the two-phonon Greens function with $q = q_1 + q_2$ and

$$\Gamma'_q(\omega) = \sum_{k\sigma, q_1, q_2} \langle\langle C_{k-q\sigma}^\dagger(t)C_{k\sigma}(t); A_{q_1}(t')A_{q_2}(t') \rangle\rangle_\omega \quad (7)$$

$$\Gamma''_q(\omega) = \sum_{k\sigma, q_1, q_2} \langle\langle A_{q_1}(t)A_{q_2}(t); C_{k+q\sigma}^\dagger(t')C_{k\sigma}(t') \rangle\rangle_\omega \quad (8)$$

are the mixed response functions. The phonon spectrum will depend on the two-particle Green's functions χ , Γ , Γ' and Γ'' which will have different features in the normal and in the CDW phases and hence should be evaluated separately. However, as can be seen from (7) and (8) the mixed Green's functions Γ' and Γ'' will contribute only in higher orders in the coupling constants g and α as compared to χ and Γ . Hence in evaluating the phonon self-energy we neglect Γ' and Γ'' .

As mentioned in § 1 the scattering of electromagnetic radiation proceeds through the excitation of electron-hole pairs which in turn excite phonons via electron-phonon coupling. Thus the single phonon excitation associated with the Raman scattering process has to involve a phonon with zero wave vector. Hence ultimately the phonon self-energy and consequently the quantities $\chi_q(\omega)$ and $\Gamma_q(\omega)$ need to be evaluated for $q = 0$.

2.1 The normal phase

At high temperatures the layered compounds are in the normal metallic phase for which $\langle A_q \rangle = 0$. Hence the phonon self-energy is determined by $\chi_q(\omega)$ and $\Gamma_q(\omega)$. For obtaining the self-energy to lowest order in α and g we need to evaluate the electron response function $\chi_q(\omega)$ only for free electrons which is given by

$$\chi_q^0(\omega) = \sum_{k\sigma} \frac{n_{k-q\sigma} - n_{k\sigma}}{\omega + \varepsilon_{k-q} - \varepsilon_k}, \quad (9)$$

where

$$n_{k\sigma} \equiv \langle C_{k\sigma}^\dagger C_{k\sigma} \rangle = [\exp(\beta\varepsilon_k) + 1]^{-1} \quad (10)$$

is the Fermi function. As is well known in the case of metals $\chi_q^0(\omega)$ is responsible for the Kohn anomaly observed at $q = 2k_F$ (k_F being the Fermi wave vector) in the phonon dispersion curve. In low-dimensional systems (due to nesting of the Fermi surface) $\chi_q^0(\omega)$ gives rise to the giant Kohn anomaly where the $q = 2k_F$ phonon shows pronounced softening on lowering the temperature resulting in the instability of the lattice and the consequent Peierls-Fröhlich transition (Toombs 1978) to the CDW state.

On the other hand, in order to incorporate temperature-dependence of two-phonon modes, we have to calculate the two-phonon Green's function $\Gamma_q(\omega)$ in the presence of electron-phonon interaction using the Hamiltonian given by (1a) without the anharmonic term. On carrying out the calculation to lowest order in the coupling constants α and g and keeping in mind the fact that ultimately our interest lies in Raman scattering where only the $q = 0$ (i.e. $q_2 = -q_1$) phonon is involved, we obtain

$$\Gamma_0(\omega) = \frac{4\omega}{\pi} \sum_{q_1} \omega_{q_1} N_{q_1} [\omega(\omega^2 - 4\omega_{q_1}^2) - 2g^2 \omega_{q_1} \{4\omega\chi_{q_1}^{(1)}(\omega) + (\omega^2 + 4\omega_{q_1}^2)\chi_{q_1}^{(2)}(\omega)\}]^{-1} \quad (11)$$

with

$$\chi_q^{(1)}(\omega) = \sum_{k\sigma} \frac{(n_{k-q\sigma} - n_{k\sigma})(\omega + \varepsilon_{k-q} - \varepsilon_k)}{(\omega + \varepsilon_{k-q} - \varepsilon_k)^2 - \omega_q^2}, \quad (12)$$

$$\chi_q^{(2)}(\omega) = \sum_{k\sigma} \frac{n_{k-q\sigma} - n_{k\sigma}}{(\omega + \varepsilon_{k-q} - \varepsilon_k)^2 - \omega_q^2}, \quad (13)$$

and

$$N_q = 2\nu_q + 1, \quad (14)$$

where

$$\nu_q = [\exp(\beta\omega_q) - 1]^{-1} \quad (15)$$

is the Bose function. The details of the derivation of (11) and the approximations involved therein are given in Appendix-A.

The substitution of $\chi_q^0(\omega)$ and $\Gamma_q(\omega)$ in (4) gives the phonon self-energy $\Sigma_q(\omega)$. However, as pointed out earlier the Raman scattering process involves only the $q = 0$ phonon, for which $\chi_q^0(\omega)$ vanishes as can be seen from (9) and hence $\Sigma_0(\omega)$ is entirely given by $\Gamma_0(\omega)$.

So far, the fact that the systems under consideration have low-dimensionality has not been invoked explicitly. For these systems the electronic spectrum possesses electron-hole symmetry and the Fermi surface exhibits nesting property when translated by a

wave vector Q ($= \pm 2k_f$) i.e.,

$$\varepsilon_{k \pm Q} = -\varepsilon_k \quad (16)$$

The nesting is perfect for one-dimensional systems, whereas for two-dimensional systems it is satisfied only along certain directions of the wave vectors. In view of the importance of the wave vector Q , the sum over q_1 in (11) can be divided into two parts, (i) the region with wave vectors $\pm Q$ and (ii) the rest of the q_1 space. Again it is well known that for wave vectors other than Q the effect of the electron-phonon interaction is only to produce a small shift in the phonon frequency. Hence the contribution of the electron-phonon interaction can be neglected in the term with $q_1 \neq Q$. This approximation is similar to the one used by Bilbro and Mc Millan (1976) for A15 compounds. With this we can write (11) as

$$\Gamma_0(\omega) = \frac{4}{\pi} \left[\frac{3 \times 2 \omega \omega_Q N_Q}{\omega(\omega^2 - 4\omega_Q^2) - 2g^2 \omega_Q \{4\omega \chi_Q^{(1)}(\omega) + (\omega^2 + 4\omega_Q^2) \chi_Q^{(2)}(\omega)\}} + \sum_{q_1 \neq Q} \frac{\omega_{q_1} N_{q_1}}{(\omega^2 - 4\omega_{q_1}^2)} \right] \quad (17)$$

The factors 2 and 3 in the first term are included because of the fact that the contributions of $+Q$ and $-Q$ are same and that there are three equivalent directions along which nesting is satisfied in the case of layered compounds: the transition metal dichalcogenides (Klein 1982a).

The evaluation of $\chi_Q^{(1)}(\omega)$ and $\chi_Q^{(2)}(\omega)$ can be carried out in the usual static approximation (i.e. $\omega = 0$) and neglecting ω_q in the denominators of (12) and (13) (which is justified since the phonon frequencies are very small compared to any structure in the electronic energy spectrum). Thus using the nesting property (equation (16)) we have

$$\chi_Q^{(1)}(\omega) \approx \chi_Q^{(1)}(0) = -N(0) \int_{-E_B}^{E_B} d\varepsilon \frac{\tanh(\beta\varepsilon/2)}{\varepsilon} = 2N(0) \ln \left(\frac{k_B T}{1.14 E_B} \right) \quad (18)$$

and $\chi_Q^{(2)}(\omega) = 0$ (odd integral), where $N(0)$ is the electron density of states at the Fermi level and the cut-off E_B determines the region around the Fermi level within which nesting property holds good.

In order to evaluate the integral in the second term of (17) explicitly we approximate N_{q_1} by an average \bar{N}_{q_1} . Since we are interested in q_1 values around Q we can assume

$$\bar{N}_{q_1} \approx N_Q = \coth(\beta\omega_Q/2)$$

and use the Debye dispersion for ω_{q_1} . When the resultant expression along with (18) is substituted in (17), the phonon self-energy becomes

$$\Sigma_0(\omega) = 36\pi\alpha^2\omega_0\Gamma_0(\omega) \quad (19a)$$

$$= 432\alpha^2\omega_0 \coth\left(\frac{\beta\omega_Q}{2}\right) \left\{ \frac{2\omega_Q}{\omega^2 - 4\Omega_Q^2(T)} - \frac{1}{8\omega_D} \left[1 + \frac{1}{4} \left(\frac{\omega}{\omega_D} \right)^2 \ln \left(1 - 4 \left(\frac{\omega}{\omega_D} \right)^{-2} \right) \right] \right\}, \quad (19b)$$

where ω_D is the Debye frequency, ω_0 is the frequency of the $q = 0$ Raman-active phonon, ω_Q the frequency of the original (unperturbed) acoustic phonon at $q = Q$ and Ω_Q is the usual Kohn anomaly phonon (soft mode) frequency given by

$$\Omega_Q^2(T) = s\omega_Q^2 \ln(T/T_p) \quad (20)$$

with the dimensionless coupling constant

$$s = 4g^2 N(0)/\omega_Q \quad (20a)$$

and the Peierls transition temperature

$$T_p = 1.14 E_F k_B^{-1} \exp(-1/s). \quad (20b)$$

Equation (20b) is obtained from the condition that at T_p the soft mode frequency goes to zero. It is obvious from (19b) that the phonon self-energy has a pole around $2\Omega_Q$. This would appear as a two-phonon peak in the phonon spectral function with frequency twice that of the Kohn anomaly phonon and (according to (20)) will show strong softening with decreasing temperature. The self-energy has also a logarithmic singularity at $\omega = 2\omega_D$. Since $\omega_Q \sim \omega_D$, this will more or less superpose with the $2\Omega_Q$ peak and hence provide a width to it in the phonon spectral function. Thus it appears that the characteristics of this anharmonicity-mediated two-phonon mode would be similar to the one observed in the Raman scattering experiment.

2.2 The CDW phase

The low-dimensional systems undergo Peierls transition on lowering the temperature below T_p . In this state electrons and holes having the same spin but different wave vectors k and $k + Q$ are correlated so that the Q th component of the electronic charge density $\rho_Q \left(= -e \sum_{k\sigma} \langle C_{k+Q\sigma}^\dagger C_{k\sigma} \rangle \right)$ acquires a finite value. This leads to a periodic modulation of the charge density with the wave vector Q accompanied by a static lattice distortion which opens up a gap in the electronic energy spectrum at the Fermi level along the direction of Q . Thus the CDW instability gives rise to a displacive phase transition wherein phonons of wave vector $\pm Q$ (the Kohn anomaly phonons) condense and execute new quasi-harmonic vibrations about the displaced positions. These new phonons are the so-called CDW-amplitude modes (CDW-AM) which appear at $q = 0$ in the zone-folded spectrum, and thus acquire Raman activity. Since these modes originate from the Kohn anomaly phonons their frequencies are much less compared to those of the normal optic phonons of the system. As mentioned in §1, the Raman spectra of the layered compounds in the CDW-phase also show broad features identified as two-phonon modes besides the CDW-AM and the normal optic phonons. The frequencies of these two-phonon modes are around twice those of the Kohn anomaly phonons and increase with decreasing temperature unlike their temperature-dependence in the normal phase. These features can again be explained on the basis of anharmonic interactions. The self-energy of the system in the CDW phase will still be given by (4); however $\langle A_q \rangle$, χ_q and Γ_q have to be evaluated with the replacement of the free electron term by H_{CDW} which describes electrons in the CDW state. In the meanfield approximation H_{CDW} is given by (Balseiro and Falicov 1979)

$$H_{\text{CDW}} = \sum_{k\sigma} \varepsilon_k C_{k\sigma}^\dagger C_{k\sigma} - G_0 \sum_{k\sigma} C_{k+Q\sigma}^\dagger C_{k\sigma} - G_1 \sum_{k\sigma}'' C_{k+Q\sigma}^\dagger C_{k\sigma} + G_0 G_1 / \lambda, \quad (21)$$

where

$$G_0 = \lambda \sum_k'' \langle C_{k+Q}^\dagger C_k \rangle, \quad (22a)$$

$$G_1 = \lambda \sum_k \langle C_{k+Q}^\dagger C_k \rangle, \quad (22b)$$

λ being the effective strength of the electron-electron interaction mediated by phonons and the doubly-primed summation is over the states which satisfy the two conditions

$$|\varepsilon_k - \varepsilon_F| < \omega_D \quad \text{and} \quad |\varepsilon_{k+Q} - \varepsilon_F| < \omega_D. \quad (23)$$

The quantities G_0 and G_1 are related to the energy gap in the electron spectrum.

The electron response function $\chi_q(\omega)$ evaluated with H_{CDW} becomes

$$\begin{aligned} \chi_q(\omega) = & \frac{1}{2\pi} \sum_{k\sigma} \{ [\omega^2 - E_+^2(k, q)] [\omega^2 - E_-^2(k, q)] \}^{-1} \\ & \times \{ \phi_0(k, q) [(\omega + \varepsilon_k + \varepsilon_{k-q})((\omega - \varepsilon_{k-q})^2 - E_k^2) \\ & - (\omega - \varepsilon_k - \varepsilon_{k-q})G_{k-q}^2 - \phi_1(k, q)G_k [(\omega - \varepsilon_{k-q})^2 - E_k^2 + G_{k-q}^2] \\ & - \phi_2(k, q)G_{k-q} [(\omega + \varepsilon_k)^2 - E_{k-q}^2 + G_k^2] \\ & - 2\omega\phi_3(k, q)G_k G_{k-q} \}, \quad (24) \end{aligned}$$

where

$$G_k = \begin{cases} G_0 + G_1 & \text{(if condition (23) is satisfied)} \\ G_0 & \text{(otherwise),} \end{cases} \quad (25)$$

$$E_k^2 = \varepsilon_k^2 + G_k^2, \quad (26)$$

$$E_\pm(k, q) = E_k \pm E_{k-q}, \quad (27)$$

$$\phi_0(k, q) = n_{k-q\sigma} - n_{k\sigma}, \quad (28a)$$

$$\phi_1(k, q) = \langle C_{k-q\sigma}^\dagger C_{k-q-Q\sigma} \rangle - \langle C_{k\sigma}^\dagger C_{k-Q\sigma} \rangle, \quad (28b)$$

$$\phi_2(k, q) = \langle C_{k-q+Q\sigma}^\dagger C_{k-q\sigma} \rangle - \langle C_{k+Q\sigma}^\dagger C_{k\sigma} \rangle, \quad (28c)$$

$$\phi_3(k, q) = \langle C_{k-q+Q\sigma}^\dagger C_{k-q-Q\sigma} \rangle - \langle C_{k+Q\sigma}^\dagger C_{k-Q\sigma} \rangle. \quad (28d)$$

In deriving (24) as well as in what follows we use the nesting property (equation (16)) and assume that $k \pm 2Q = k$. The equal time correlation functions $n_{k\sigma}$ and $\langle C_{k\sigma}^\dagger C_{k-Q\sigma} \rangle$ which can be calculated by evaluating the single-particle electron Green functions in the CDW phase are given by

$$n_{k\sigma} = \frac{1}{2} \left[1 - \frac{\varepsilon_k}{E_k} \tanh \frac{\beta E_k}{2} \right], \quad (29)$$

and

$$\langle C_{k\sigma}^\dagger C_{k-Q\sigma} \rangle = \frac{G_k}{2E_k} \tanh \frac{\beta E_k}{2}. \quad (30)$$

The expression for $\chi_q(\omega)$ as given by (24) is valid for any q . However, as pointed out earlier, Raman scattering requires $q = 0$. But in the CDW state the wave vector Q is a reciprocal lattice vector which when zone-folded coincides with the zone-centre, $q = 0$. Hence in the low temperature phase we choose $q = Q$ for the analysis of the phonon Raman spectrum. In this special case

$$G_{k-Q} = G_k, \quad E_{k-Q} = E_k \quad \text{and} \quad E_-(k, Q) = 0,$$

and (24) reduces to

$$\chi_Q(\omega) = \frac{1}{\pi\omega} \sum_k \frac{\varepsilon_k [\omega(\omega + 2\varepsilon_k) - 8G_k^2] \tanh \frac{\beta E_k}{2}}{E_k(\omega^2 - 4E_k^2)}. \quad (31)$$

Since E_k is an even function of ε_k ,

$$\chi_Q(\omega) = \frac{2N(0)}{\pi} \int_{-E_B}^{E_B} d\varepsilon_k \frac{\varepsilon_k^2 \tanh \frac{\beta E_k}{2}}{E_k(\omega^2 - 4E_k^2)}, \quad (31a)$$

which when evaluated at zero-temperature becomes

$$\chi_Q(\omega) = \frac{N(0)}{\pi} \left[\frac{(4G^2 - \omega^2)^{1/2}}{\omega} \tan^{-1} \frac{\omega}{(4G^2 - \omega^2)^{1/2}} - \ln \left(\frac{2E_B}{G} \right) \right]. \quad (32)$$

The cut-off E_B determines the energy range within which nesting property holds good. Moreover it has been assumed that $G_0 = G_1 = G/2$ ($2G$ being the CDW energy gap) and that $E_B \gg G$. Equation (32) clearly shows that the phonon self-energy will have a square-root singularity at $\omega = 2G$ which will develop into the CDW amplitude mode.

In order to calculate the phonon self-energy it is further necessary to evaluate the two-phonon Green's function $\Gamma_q(\omega)$ in the CDW state and as argued earlier for Raman scattering we would choose $q = Q$ which is equivalent to $q = 0$. To be more accurate we should once again calculate $\Gamma(\omega)$ with electron-phonon interaction where electrons are described by H_{CDW} . However, for simplicity, we assume that $\Gamma_Q(\omega)$ in the CDW phase would be similar to $\Gamma_0(\omega)$ in the normal phase with the Kohn anomaly phonon replaced by the corresponding one in the CDW state. Thus we have

$$\Gamma_Q(\omega) = \frac{4N_Q}{\pi} \left\{ \frac{6\omega_Q}{\omega^2 - 4\tilde{\Omega}_Q^2} + \sum_{q_1 \neq Q} \frac{\omega_{q_1}}{(\omega^2 - 4\omega_{q_1}^2)} \right\}, \quad (33)$$

where $\tilde{\Omega}_Q$ is the frequency of the Kohn anomaly phonon in the CDW phase and is known (Rietschel 1973) to increase with lowering temperature. Hence (in analogy with (20)) for zero temperature we can write $\tilde{\Omega}_Q^2 = \eta\omega_Q^2$, $\eta < 1$ being a constant. The first term in (33) shows that the phonon self-energy will have a pole at $\omega = 2\tilde{\Omega}_Q$ which will shift to higher frequency with decreasing temperature and the second term will provide a width to it.

Thus the nature of this mode will be similar to that of the experimentally observed two-phonon mode in the CDW phase.

Finally at low temperatures the quantity $\langle A_q \rangle$ will be non-zero for $q = Q$ having a constant value proportional to the CDW gap and will be given by $\langle A_Q \rangle = G/g$ (Berlinsky 1979). Therefore substituting $\langle A_Q \rangle$, $\chi_Q(\omega)$ and $\Gamma_Q(\omega)$ into (4) we obtain the phonon self-energy in the CDW phase at zero temperature as

$$\begin{aligned} \Sigma_Q(\omega) = 4\omega_Q \left\{ 3\alpha G/g + g^2 N(0) \left[\frac{(4G^2 - \omega^2)^{1/2}}{\omega} \tan^{-1} \frac{\omega}{(4G^2 - \omega^2)^{1/2}} \right. \right. \\ \left. \left. - \ln \left(\frac{2E_B}{G} \right) \right] + 216\alpha^2 \left[\frac{\omega_Q}{\omega^2 - 4\tilde{\Omega}_Q^2} \right. \right. \\ \left. \left. - \frac{1}{16\omega_D} \left\{ 1 + \frac{1}{4} \left(\frac{\omega}{\omega_D} \right)^2 \ln \left(1 - 4 \left(\frac{\omega}{\omega_D} \right)^2 \right) \right\} \right] \right\}. \end{aligned} \quad (34)$$

It is obvious from (34) that the phonon spectral function in the CDW phase will have additional peaks around $\omega = 2G$ and $\omega = 2\tilde{\Omega}_Q$ corresponding to the CDW amplitude mode and the two-phonon mode respectively (besides the one around ω_Q) having similar features as observed experimentally.

3. Results and discussion

We have evaluated the phonon self-energy in the normal and in the CDW phases. In order to compare the results with experiments it is necessary to know the phonon spectral function (which one measures in Raman scattering) $S_q(\omega) = 2 \text{Im} D_q(\omega)$. This can be calculated by providing a phenomenological width γ_0 to the phonons with the replacement $\omega^2 \rightarrow \omega^2 - 2i\omega\gamma_0$.

3.1 Spectral function in the normal state

The phonon Green's function $D_q(\omega)$ in the normal state is obtained by substituting (19) in (3). Hence the spectral function is given by

$$S_0(x) \propto \frac{2\tilde{\gamma}_0 \tilde{\omega}_Q^2 x + \gamma_1(x)}{[\tilde{\omega}_Q^2 x^2 - 1 - F_0(x)]^2 + [2\tilde{\gamma}_0 \tilde{\omega}_Q^2 x + \gamma_1(x)]^2}, \quad (35)$$

where

$$\begin{aligned} F_0(x) = 432t^2 \tilde{\omega}_Q \coth(K\tilde{T})^{-1} \\ \times \left\{ \frac{2}{x^2 - 4s \ln \tilde{T}} - \frac{r}{8} \left[1 + \frac{1}{4} r^2 x^2 \ln \left| 1 - \frac{4}{r^2 x^2} \right| \right] \right\} \end{aligned} \quad (36)$$

$$\gamma_1(x) = \begin{cases} \frac{27\pi}{2} t^2 r^3 \tilde{\omega}_Q x^2 \coth(K\tilde{T})^{-1} & \text{for } x < 2/r \\ 0 & \text{for } x > 2/r \end{cases} \quad (37a)$$

$$(37b)$$

with

$$\begin{aligned} x = \omega/\omega_Q, \quad \tilde{\gamma}_0 = \gamma_0/\omega_Q, \quad \tilde{\omega}_Q = \omega_Q/\omega_0, \quad \tilde{T} = T/T_p, \\ K = 2k_B T_p/\omega_Q, \quad r = \omega_Q/\omega_D, \quad t = \alpha/\omega_Q, \end{aligned} \quad (38)$$

and s is as defined in (20). The dimensionless electron-phonon and anharmonic coupling constants s and t as well as the phenomenological width $\tilde{\gamma}_0$ are the three parameters in the theory. On the other hand the quantities $\tilde{\omega}_0$, K and r can be determined from the experimental data for a given compound.

The phonon excitation spectrum is determined from the solution of the equation

$$\tilde{\omega}_0^2 x^2 - 1 - F_0(x) = 0, \quad (39)$$

whose roots will show up as peaks in the spectral function. It is evident from (39) and (36) that there are three roots with frequencies around (i) $x \sim \tilde{\omega}_0^{-1}$ corresponding to the bare optical phonon (ii) $x \sim 2(s \ln \tilde{T})^{1/2}$, corresponding to the two-phonon peak at twice the Kohn anomaly phonon frequency and finally (iii) $x \sim 2/r$ which arises from the logarithmic singularity at $\omega = 2\omega_D$. It can be easily seen from (35) and (37) that the anharmonic interaction generates an additional temperature-dependent width $\gamma_1(x)$ for $x < 2/r$ (i.e. $\omega < 2\omega_D$). An approximate solution of (39) is given in Appendix-B.

We evaluate the phonon spectral function numerically for the representative system 2H-NbSe₂ with the following bare values of the parameters. For this compound $\omega_0 = 230 \text{ cm}^{-1}$, $\omega_D = 100 \text{ cm}^{-1}$, $\omega_D = 110 \text{ cm}^{-1}$ and $T_p = 33 \text{ K}$. The values of ω_0 and ω_D are taken from the neutron scattering data (Moncton *et al* 1977). The other parameters $\tilde{\gamma}_0 = 0.072$, $s = 0.516$ and $t = 0.012$ are chosen so as to obtain the original Raman active phonon and the two-phonon mode around the experimentally observed frequencies. Although the figures are plotted for 2H-NbSe₂, the qualitative features will remain the same for other layered materials (e.g. 2H-TaSe₂) with appropriate changes in the parameters.

Figure 1 shows the phonon spectral function for two different temperatures $\tilde{T} = 3$ and 9 (which correspond to $\sim 100 \text{ K}$ and $\sim 300 \text{ K}$ respectively). The following features can be clearly noticed from the figure. (i) The frequencies of the two-phonon modes for $\tilde{T} = 9$ and 3 are 194 and 146 cm^{-1} whereas the experimental values are 180 and 160 cm^{-1} respectively. Thus the theory explains the decrease in the two-phonon frequency with decreasing temperature. (ii) For the above temperatures the calculated optic phonon frequencies are 247 and 234 cm^{-1} the experimental value being around 240 cm^{-1} which is not very sensitive to temperature. (iii) The intensity of the two-phonon peak at high temperature is comparable to that of the single optic phonon peak and decreases with lowering temperature in conformity with experimental data. This result is of particular importance since the Maldague-Tsang mechanism for enhancing the intensity of two-phonon mode is not invoked in the present calculation. (iv) The intensity of the high frequency optic phonon increases with decreasing temperature which agrees with experimental data for 2H-TaSe₂ (Sugai and Murase 1982). (v) A small dip appears at the frequency $2\omega_D$ as expected from the logarithmic singularity at $x = 2/r$. This becomes inconspicuous at higher temperatures.

The effect of varying the parameters s and t is shown in figures 2 and 3. The spectral function for two different values of the anharmonic interaction ($t = 0.012$ and 0.02) at $\tilde{T} = 9$ is plotted in figure 2. It can be clearly seen that on increasing t , (i) the frequency of the two-phonon mode decreases and that of the optic phonon increases, (ii) the width of the two-phonon peak increases as expected from (37) and (iii) the intensity of the single phonon peak decreases whereas that of the two-phonon peak increases slightly. This is natural since the two-phonon mode arises due to anharmonic interaction.

Figure 3 depicts the spectral function for two different values of the electron-phonon

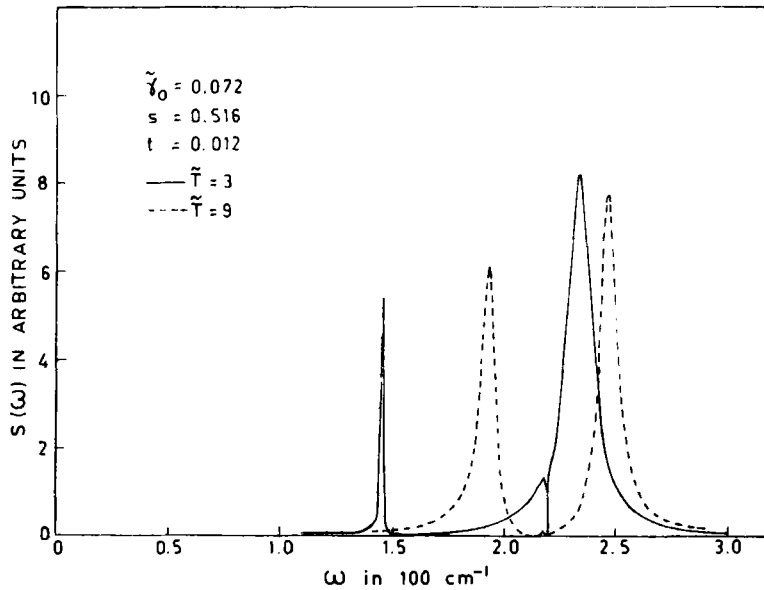


Figure 1. Phonon spectral function in the normal phase for two temperatures. The solid curve is for $\tilde{T} = 3$ and the broken curve for $\tilde{T} = 9$ which correspond to nearly 100 K and 300 K respectively. The first peak in each curve is the two-phonon mode whose frequency increases with increasing temperature. The high-frequency peak corresponds to the original optic phonon in the system.

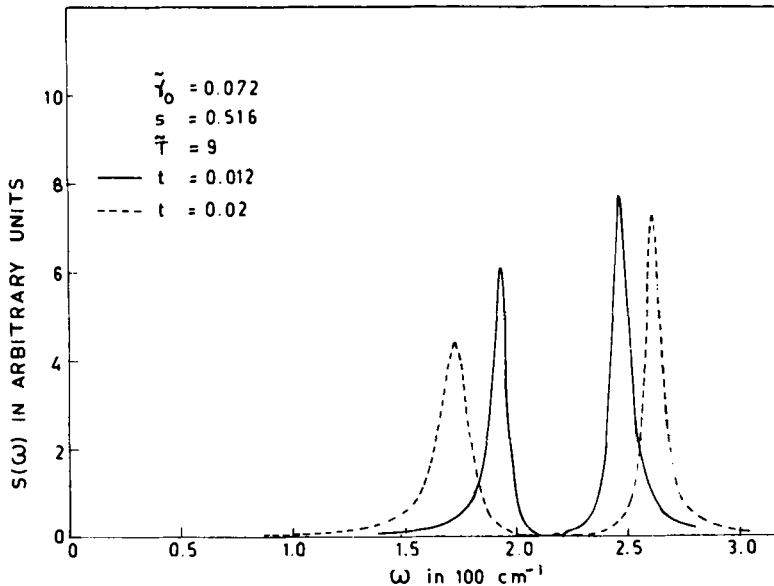


Figure 2. Effect of variation of anharmonic parameter on the phonon spectral function in the normal phase. The solid curve is for $t = 0.012$ and the broken curve for $t = 0.02$. On increasing anharmonicity the frequency of the two-phonon mode decreases whereas that of the original optic phonon increases.

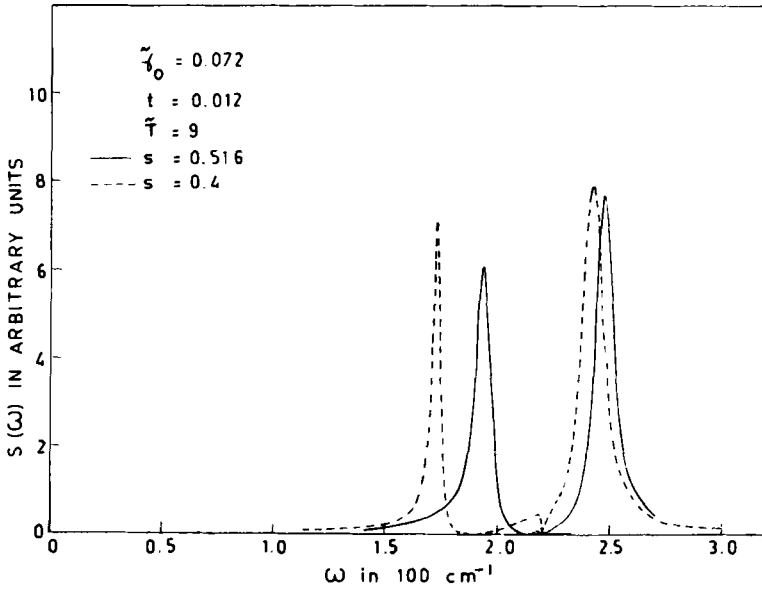


Figure 3. Effect of changing electron-phonon coupling strength on the phonon spectral function in the normal phase. The solid curve is for $s = 0.516$ and the broken curve for $s = 0.4$. On decreasing s the frequency and strength of the two-phonon mode decreases drastically whereas there is a small change in the original optic phonon.

coupling constant ($s = 0.516$ and 0.4) at $T = 9$. It is evident from the figure that on decreasing s , (i) the two-phonon mode frequency decreases by a large amount whereas the optic mode frequency decreases slightly, (ii) there is a small increase in the intensity of the optic phonon and decrease in that of the two-phonon peak, (iii) the width of the two-phonon peak decreases and that of the optic phonon shows slight increase and (iv) the dip at $2\omega_D$ becomes more prominent with decreasing s . The pronounced change in the two-phonon mode on varying the electron-phonon coupling is expected since it depends on the Kohn anomaly phonon whose frequency is directly proportional to \sqrt{s} (equation (25)).

The above qualitative features are also understood from the approximate solution of (39) given in Appendix-B.

3.2 Spectral function in the CDW state

In the CDW phase the phonon spectral function at zero temperature is obtained by substituting (34) into (3) and is given by

$$S(y) \propto \frac{2\tilde{\gamma}_0 \tilde{G} y + \gamma_1(y) + \gamma_2(y)}{[\tilde{G}^2 y^2 - 1 - F_1(y) - F_2(y)]^2 + [2\tilde{\gamma}_0 \tilde{G} y + \gamma_1(y) + \gamma_2(y)]^2}, \quad (40)$$

where

$$F_1(y) = 4 \left\{ \left[\frac{3}{2} R \tilde{G} - \frac{1}{4} s \ln(4 \tilde{E}_B / \tilde{G}) \right] + 216 t^2 \left[(\tilde{G}^2 y^2 - 4\eta)^{-1} - \frac{r}{16} \left(1 + \frac{1}{4} r^2 \tilde{G}^2 y^2 \ln \left| 1 - \frac{4}{r^2 \tilde{G}^2 y^2} \right| \right) \right] \right\}, \quad (41a)$$

$$F_2(y) = \begin{cases} s \frac{(1-y^2)^{1/2}}{y} \tan^{-1} \frac{y}{(1-y^2)^{1/2}} & \text{for } y < 1, \\ s \frac{(y^2-1)^{1/2}}{y} \tanh^{-1} \frac{(y^2-1)^{1/2}}{y} & \text{for } 1 < y < \frac{2}{\tilde{G}r}, \end{cases} \quad (41b)$$

$$\gamma_1(y) = \frac{27\pi}{2} t^2 r^3 \tilde{G}^2 y^2, \quad (42)$$

$$\gamma_2(y) = \begin{cases} 0 & \text{for } y < 1 \end{cases} \quad (43a)$$

$$\begin{cases} 2\pi s (y^2-1)^{1/2}/y & \text{for } 1 < y < \frac{2}{\tilde{G}r}, \end{cases} \quad (43b)$$

with

$$y = \omega/2G, \quad \tilde{E}_B = E_B/\omega_Q, \quad \tilde{G} = 2G/\omega_Q \quad \text{and} \quad R = \alpha/g, \quad (44)$$

the other quantities being the same as defined in (38). Since the two-phonon mode frequency is expected to be less than $2\omega_D$, we do not consider the region beyond $2\omega_D$. As usual the frequencies associated with the phonon-like excitations in the system are given by

$$\tilde{G}^2 y^2 - 1 - F_1(y) - F_2(y) = 0. \quad (45)$$

From the structure of (41) it is expected that (45) will have four roots, (i) $y \sim \tilde{G}^{-1}$ which corresponds to the original phonon (ω_Q) in the system (ii) $y \sim 1$ which is the CDW amplitude mode having frequency around the CDW gap ($2G$), (iii) $y \sim 2\sqrt{\eta/\tilde{G}}$ corresponding to the two-phonon mode around twice the Kohn anomaly phonon frequency and finally (iv) $y \sim 2/(r\tilde{G})$ which arises from the logarithmic singularity at $2\omega_D$. It is clear from (40) and (43) that the spectral function acquires an extra width $\gamma_2(y)$ in the region $2G < \omega < 2\omega_D$ because of the electron-phonon-interaction in addition to $\gamma_1(y)$, the width generated by the anharmonic interaction. The additional width will affect only the two-phonon mode and not the CDW-AM as the latter lies below $2G$. Thus the two-phonon mode in the CDW state is expected to be more broadened than in the normal state, which agrees with the experimental findings (Sugai and Murase 1982).

The spectral function in the CDW state is calculated numerically for 2H-NbSe_2 and plotted in figures 4–7. The values of the different parameters used are $\tilde{\gamma}_0 = 0.1$, $R = 0.13$, $E_B = 400 \text{ cm}^{-1}$, $2G = 80 \text{ cm}^{-1}$, $\eta = 0.65$, $s = 0.4$ and $t = 0.038$. The other quantities, ω_Q , ω_D have the same values as in the normal phase. These values are so chosen as to obtain agreement with the experimental data on the frequencies of CDW-AM and the two-phonon modes at zero temperature.

In figure 4 $S(\omega)$ is plotted for two different values of the width parameter namely $\tilde{\gamma}_0 = 0.1$ and 0.2 . The spectral function shows three peaks. The prominent low frequency peak is the CDW-AM which is around the experimentally observed value of 40 cm^{-1} . The high frequency (178 cm^{-1}) peak corresponds to the two-phonon mode whose frequency at zero temperature is expected to be nearly equal to its room temperature value in the normal phase (figure 8 of Sugai and Murase 1982). The two-phonon peak is much more broadened in the CDW phase than in the normal phase, and is much weaker compared to the CDW-AM, which is borne out experimentally (Sugai and Murase 1982). As pointed out earlier there should be a peak corresponding to the

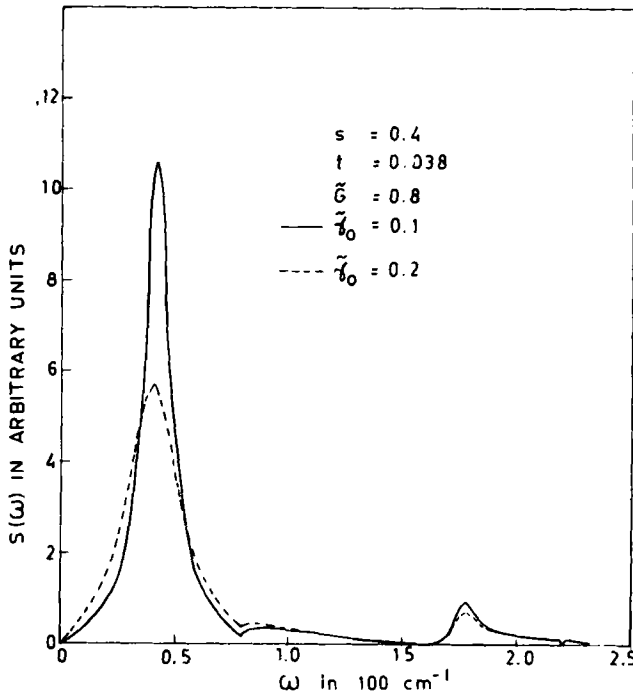


Figure 4. Phonon spectral function in the CDW phase at zero temperature for two values of the bare width. The solid curve is for $\tilde{\gamma}_0 = 0.1$ and the broken curve for $\tilde{\gamma}_0 = 0.2$. The sharp low frequency peak in each curve is the CDW-amplitude mode and the broad high frequency peak is the two-phonon mode. The middle peak which corresponds to the original phonon with wave vector Q appears to be highly suppressed.

original phonon with frequency $\sim \omega_Q$, which although present in figure 4 appears to be very much suppressed. This is because in the CDW phase almost all the strength of this phonon is transferred to the CDW-AM. Besides all these peaks there should also be a dip corresponding to the logarithmic singularity at $2\omega_D$, which is rather insignificant in figure 4.

Figure 4 also shows the effect of the variation of the bare width $\tilde{\gamma}_0$ on the spectral function. It is clear that increasing the width reduces the strengths of the CDW-AM and two-phonon modes without altering their frequencies. The reduction in the strength of the CDW-AM is accompanied by a small but finite increase in the strength of the original ω_Q peak. This phenomenological variation in the width can represent the effect of non-magnetic impurities on the CDW-state, the reduction of the strength of the CDW-AM on increasing $\tilde{\gamma}_0$ being the signature for the suppression of the CDW-state by these impurities. This is similar to the effect of magnetic impurities on the superconducting gap excitation mode in 2H-NbSe₂ (Sooryakumar *et al* 1981).

The effect of changing the anharmonic parameter is depicted in figure 5 for $t = 0.035$ and 0.042 . It is evident from the plots that on decreasing t , the frequency of the CDW-AM increases while that of the two-phonon mode decreases slightly and that the width of CDW-AM increases. This is easy to understand since according to (42), the width $\gamma_1(y)$ due to anharmonicity is proportional to $(ty)^2$ and thus the decrease in t is over-compensated by the increase in the frequency y .

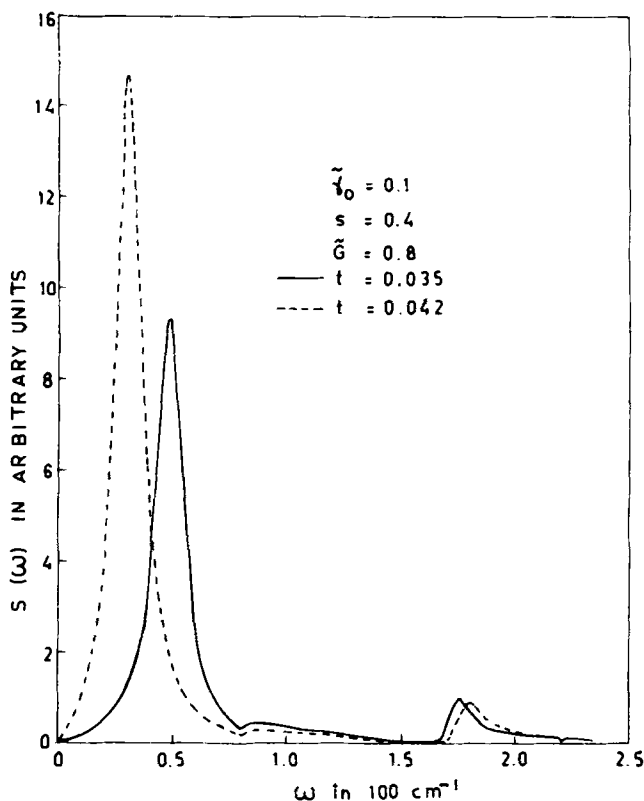


Figure 5. Effect of variation of anharmonic parameter on the phonon spectral function in the CDW phase. The solid curve and the broken curve correspond to $t = 0.035$ and 0.042 respectively. With increasing anharmonicity the frequency of CDW-AM decreases and that of two-phonon mode increases.

In figure 6 we show the variation of the spectral function with the electron-phonon coupling constant ($s = 0.28$ and 0.48). On decreasing s the frequency of the CDW-AM increases drastically but the two-phonon mode frequency increases slightly. Besides, there is a drastic reduction in the strength of the CDW-AM accompanied by a small increase in the strengths of the original phonon (ω_Q) and the two-phonon peaks. This is expected since the CDW transition is driven by electron-phonon interaction.

Finally figure 7 shows how $S(\omega)$ changes with the CDW gap parameter, for $\tilde{G} = 0.8$ and 0.7 . It is clear from the figure that on decreasing \tilde{G} the frequency of the CDW-AM decreases drastically, but the change in the two-phonon mode is insignificant. This is what one should expect as the CDW-AM is a direct manifestation of the magnitude of the gap in the electronic spectrum.

4. Conclusion

We have proposed a theory for the two-phonon modes observed in the Raman spectra of the layered transition metal dichalcogenides. This theory is based on the presence of anharmonic interactions in these systems. The main features of the theory are

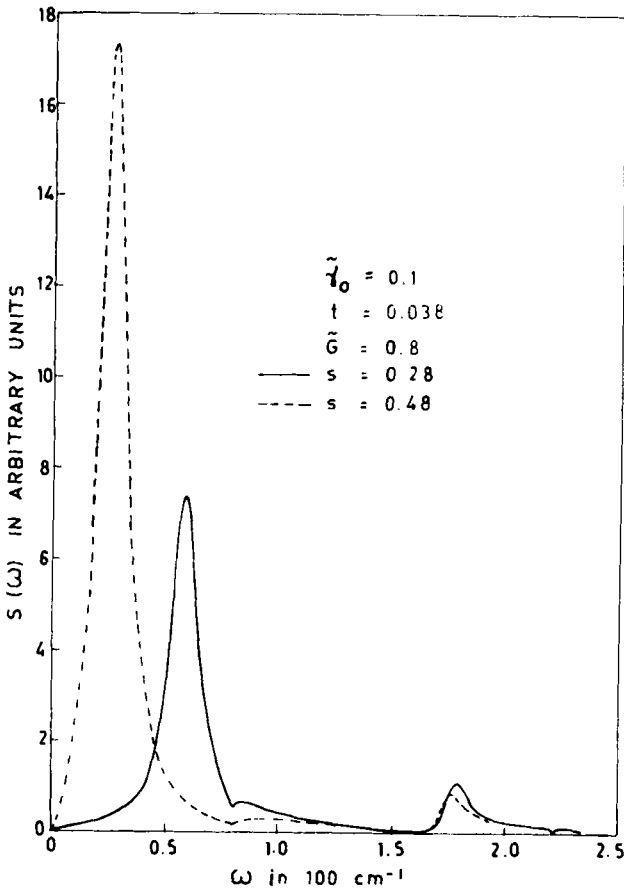


Figure 6. Effect of changing electron-phonon coupling strength on the phonon spectral function in the CDW-phase. The solid curve and the broken curve correspond to $s = 0.28$ and 0.48 respectively. On decreasing s the strength of CDW-AM decreases whereas that of two-phonon mode (and of the original phonon) increases.

summarized below. There exist anharmonicity-mediated two-phonon modes both in the normal and in the CDW phases. In the normal phase the two-phonon mode originates from the Raman-active optic phonon which couples to light through electron-hole excitation. In this phase the two-phonon Green's function which enters into the phonon self-energy is evaluated explicitly in the presence of electron-phonon interaction. It is clearly demonstrated that the frequency of the two-phonon mode is approximately twice that of the Kohn anomaly phonon and shows the observed temperature-dependence. Besides, the strength of the two-phonon peak in the spectral function is found to be comparable to that of the original optic phonon which agrees with experimental data.

In the CDW-phase the two-phonon mode is assumed to owe its origin to the phonon with wave vector Q , which when zone-folded is equivalent to $q = 0$ and becomes Raman active. In this phase the calculations are carried out for zero temperature. The two-phonon Green's function is assumed to be of the same form as in the normal phase with

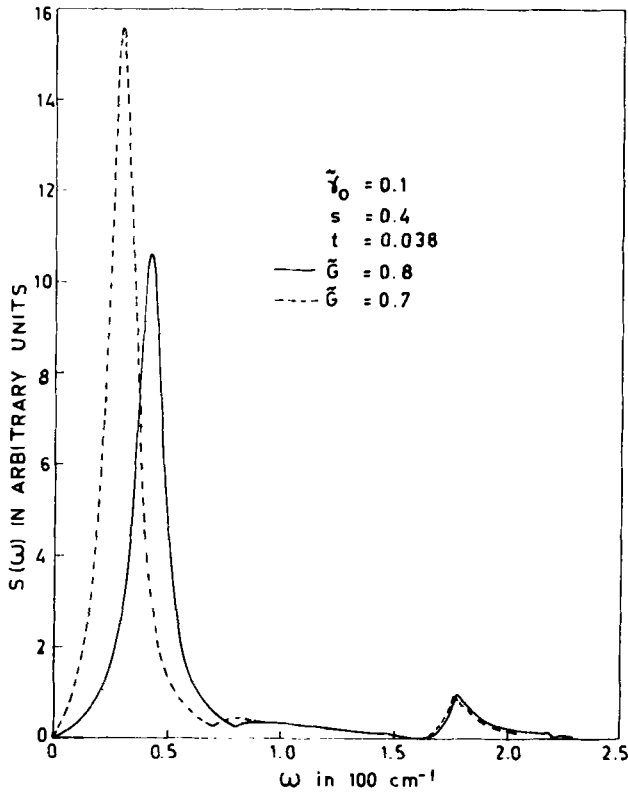


Figure 7. Effect of varying the CDW-gap parameter on the phonon spectral function. The solid curve is for $\bar{G} = 0.8$ and the broken curve for $\bar{G} = 0.7$. On decreasing \bar{G} the frequency of CDW-AM decreases and the strength of original phonon increases whereas the change in the two-phonon mode is insignificant.

the replacement of the Kohn anomaly phonon by the corresponding one in the CDW phase in a phenomenological manner. Besides the two-phonon Green's function, the phonon self-energy also involves the electron response function in the CDW phase, which is calculated explicitly and is shown to give rise to the CDW-AM phonon. Thus the spectral function shows mainly two peaks corresponding to the CDW-AM and the two-phonon mode. The latter is found to be much more broadened and weakened in strength compared to its counterpart in the normal phase.

In both the normal and CDW phases the numerical results are presented for the prototype system $2H-NbSe_2$. However the qualitative features will be the same for any other layered CDW system. Hence in discussing the results quite often reference is made to the experimental data on $2H-TaSe_2$.

We conclude the present paper by pointing out some of its shortcomings. In the normal phase the experimentally observed two-phonon mode has a large width, but the calculated peak in the spectral function appears to be rather sharp, although its intensity is comparable to the optic phonons which agrees with experiments. Our approach to the CDW phase is somewhat phenomenological. We have attributed the origin of the two-phonon mode to the phonon with wave vector Q but ignored the presence of the original high frequency Raman active mode in the system which was

considered in the normal phase. We have not calculated the two-phonon Green's function explicitly for the CDW phase and instead introduced the Kohn anomaly phonon through the parameter η in an ad hoc manner. Since the calculations are carried out for zero temperature, in the CDW phase the temperature-dependence of the two-phonon mode could not be studied. Besides, at very low temperatures the transition metal dichalcogenides are known to undergo the superconducting transition which has not been taken into account in the present calculation. A more refined calculation for the CDW phase is in progress and will be reported elsewhere.

Acknowledgement

A brief report of this work was presented at the Indo-Soviet Conference on Low Temperature Physics, Bangalore, January 1984. One of us (SNB) has benefitted from some useful discussions with Drs G K Scott and K K Bardhan at the initial stage of the work, and would like to acknowledge the hospitality of the Simon Fraser University at Canada.

Appendix-A

In order to derive equation (11) it is necessary to write down the equations of motion for the two-phonon Green's function (equation (6)) and the other related Green's functions for which we use the following notations

$$\Gamma_{q_1 q_2}^{xy}(\omega) = \langle\langle X_{q_1}(t) Y_{q_2}(t); A_{q'_1}(t') A_{q'_2}(t') \rangle\rangle_{\omega}, \quad (\text{A1})$$

and

$$\Gamma_{k-q_1, k, q_2}^x(\omega) = \langle\langle C_{k-q_1\sigma}^\dagger(t) C_{k\sigma}(t) X_{q_2}(t); A_{q'_1}(t') A_{q'_2}(t') \rangle\rangle_{\omega}, \quad (\text{A2})$$

where X, Y denote either A or B and the other indices q'_1, q'_2, σ etc are suppressed for brevity. These Green's functions have to be evaluated with electron-phonon interaction (that is, with the Hamiltonian given by (1a) except the anharmonic term) for which the equations of motion for the electron and phonon operators are given by

$$i \frac{dA_q}{dt} = \omega_q B_q, \quad (\text{A3})$$

$$i \frac{dB_q}{dt} = \omega_q A_q + 2g \sum_{k\sigma} C_{k-q\sigma}^\dagger C_{k\sigma}, \quad (\text{A4})$$

and

$$i \frac{d}{dt} (C_{k-q\sigma}^\dagger C_{k\sigma}) = (\epsilon_k - \epsilon_{k-q}) C_{k-q\sigma}^\dagger C_{k\sigma} - g \sum_q (C_{k-q+q'\sigma}^\dagger C_{k\sigma} A_{q'} - C_{k-q\sigma}^\dagger C_{k-q'\sigma} C_{q'}). \quad (\text{A5})$$

Using equations (3) to (5) we obtain the following (Fourier-transformed) equations of

motion for the Green's functions

$$(\omega^2 - \omega_{q_1}^2 - \omega_{q_2}^2) \Gamma_{q_1 q_2}^{AA}(\omega) = C(q_1 q_2) + 2\omega_{q_1} \omega_{q_2} \Gamma_{q_1 q_2}^{BB}(\omega) + 2g \sum_{k\sigma} (\omega_{q_1} \Gamma_{k-q_1, k, q_2}^A(\omega) + \omega_{q_2} \Gamma_{k-q_2, k, q_1}^A(\omega)), \quad (A6)$$

$$(\omega^2 - \omega_{q_1}^2 - \omega_{q_2}^2) \Gamma_{q_1 q_2}^{BB}(\omega) = \tilde{C}(q_1 q_2) + 2\omega_{q_1} \omega_{q_2} \Gamma_{q_1 q_2}^{AA}(\omega) + 4g \sum_{k\sigma} (\omega_{q_1} \Gamma_{k-q_2, k, q_1}^A(\omega) + \omega_{q_2} \Gamma_{k-q_1, k, q_2}^A(\omega)) - 2g \sum_{k\sigma} [(\varepsilon_{k-q_1} - \varepsilon_k) \Gamma_{k-q_1, k, q_2}^B(\omega) + (\varepsilon_{k-q_2} - \varepsilon_k) \Gamma_{k-q_2, k, q_1}^B(\omega)] - 2g^2 \sum_{k\sigma} [(n_{k\sigma} - n_{k-q_1, \sigma}) \Gamma_{q_1 q_2}^{AB}(\omega) + (n_{k\sigma} - n_{k-q_2, \sigma}) \Gamma_{q_1 q_2}^{BA}(\omega)], \quad (A7)$$

$$(\omega^2 - \omega_{q_1}^2 - \omega_{q_2}^2) \Gamma_{q_1 q_2}^{AB}(\omega) = -\omega \tilde{\tilde{C}}(q_1 q_2) + 2\omega_{q_1} \omega_{q_2} \Gamma_{q_1 q_2}^{BA}(\omega) + 2g \sum_{k\sigma} [\omega_{q_1} (\Gamma_{k-q_1, k, q_2}^B(\omega) + 2\Gamma_{k-q_2, k, q_1}^B(\omega)) - (\varepsilon_{k-q_2} - \varepsilon_k) \Gamma_{k-q_2, k, q_1}^A(\omega)] - 2g^2 \sum_{k\sigma} (n_{k\sigma} - n_{k-q_2, \sigma}) \Gamma_{q_1 q_2}^{AA}(\omega) \quad (A8)$$

where

$$C(q_1 q_2) = C_0(q_1 q_2) [\omega_{q_1} N_{q_2} + \omega_{q_2} N_{q_1}], \quad (A9)$$

$$\tilde{C}(q_1 q_2) = C_0(q_1 q_2) [\omega_{q_1} N_{q_1} + \omega_{q_2} N_{q_2}], \quad (A10)$$

$$\tilde{\tilde{C}}(q_1 q_2) = C_0(q_1 q_2) N_{q_1}, \quad (A11)$$

with

$$C_0(q_1 q_2) = \frac{1}{\pi} (\delta_{-q_1, q_1'} \delta_{-q_2, q_2'} + \delta_{-q_1, q_2'} \delta_{-q_2, q_1'}) \quad (A12)$$

and $\Gamma_{q_1 q_2}^{BA}(\omega)$ is obtained from (A8) by interchanging $q_1 \leftrightarrow q_2$ because

$$\Gamma_{q_1 q_2}^{BA}(\omega) = \Gamma_{q_2 q_1}^{AB}(\omega).$$

Similarly the equations of motion for the mixed Green's functions ((A2)) are

$$\Gamma_{k-q_1, k, q_2}^A(\omega) = C'(k, q_1 q_2) [\omega_{q_2} \Gamma_{q_1 q_2}^{AB}(\omega) + (\omega + \varepsilon_{k-q_1} - \varepsilon_k) \Gamma_{q_1 q_2}^{AA}(\omega)], \quad (A13)$$

$$\Gamma_{k-q_1, k, q_2}^B(\omega) = C'(k, q_1 q_2) [\omega_{q_2} \Gamma_{q_1 q_2}^{AA}(\omega) + (\omega + \varepsilon_{k-q_1} - \varepsilon_k) \Gamma_{q_1 q_2}^{AB}(\omega)], \quad (A14)$$

where

$$C'(k, q_1 q_2) = g(n_{k-q_1, \sigma} - n_{k\sigma}) [(\omega + \varepsilon_{k-q_1} - \varepsilon_k)^2 - \omega_{q_2}^2]^{-1}, \quad (A15)$$

and $\Gamma_{k-q_2, k, q_1}^A(\omega)$ as well as Γ_{k-q_2, k, q_1}^B are obtained from (A13) and (A14) respectively by interchanging $q_1 \leftrightarrow q_2$. In writing the above equations of motion we have decoupled some higher order Green's functions as follows

$$\begin{aligned} \langle\langle C_{k-q_1+q_2\sigma}^\dagger C_{k\sigma} A_{q_1} B_{q_2}; A_{q_1} A_{q_2} \rangle\rangle_\omega \\ \approx \delta_{q_1, q_2} n_{k\sigma} \Gamma_{q_1, q_2}^{AB}(\omega) \end{aligned} \quad (\text{A16})$$

and neglected some other Green's functions of the type

$$\langle\langle C_{k-q_1\sigma}^\dagger C_{k'\sigma'} C_{k-q_2\sigma}^\dagger C_{k\sigma}; A_{q_1} A_{q_2} \rangle\rangle_\omega,$$

because these will contribute only in higher orders in the coupling constant g . The latter approximation is consistent with the dropping of Γ' and Γ'' terms in the phonon self-energy. Thus we find that the equations of motion of all the Green's functions are coupled and hence can be solved for Γ^{AA} which we need. The result is

$$\begin{aligned} \Gamma_{q_1, q_2}^{AA}(\omega) = \frac{2}{\pi} \{ & (\omega^2 - \omega_{q_1}^2 + \omega_{q_2}^2) \omega_{q_1} N_{q_2} + (\omega^2 + \omega_{q_1}^2 - \omega_{q_2}^2) \omega_{q_2} N_{q_1} \} \\ & \times \mathcal{D}_1(q_1, q_2, \omega) - 2g^2 \omega \omega_{q_1} \omega_{q_2} \{ N_{q_1} f_4(q_2, q_1, \omega) + N_{q_2} f_4(q_1, q_2, \omega) \} \\ & \times [\mathcal{D}_1(q_1, q_2, \omega) \mathcal{D}_2(q_1, q_2, \omega) - 4g^4 \omega_{q_1} \omega_{q_2} \{ f_3(q_1, q_2, \omega) f_4(q_1, q_2, \omega) \\ & + f_3(q_2, q_1, \omega) f_4(q_2, q_1, \omega) \}]^{-1}, \end{aligned} \quad (\text{A17})$$

where

$$\mathcal{D}_1(q_1, q_2, \omega) = f(q_1, q_2, \omega) f(q_2, q_1, \omega) - 4\omega_{q_1} \omega_{q_2} f_2(q_1, q_2, \omega) f_2(q_2, q_1, \omega), \quad (\text{A18})$$

$$\begin{aligned} \mathcal{D}_2(q_1, q_2, \omega) = (\omega^2 - \omega_{q_1}^2 - \omega_{q_2}^2) [& f(q_1, q_2, \omega) + f(q_2, q_1, \omega) - (\omega^2 - \omega_{q_1}^2 - \omega_{q_2}^2)] \\ & - 4\omega_{q_1} \omega_{q_2} [\omega_{q_2} f_2(q_1, q_2, \omega) + \omega_{q_1} f_2(q_2, q_1, \omega) - \omega_{q_1} \omega_{q_2}], \end{aligned} \quad (\text{A19})$$

$$f_4(q_1, q_2, \omega) = f(q_1, q_2, \omega) f_1(q_2, q_1, \omega) + 2\omega_{q_1} f_1(q_1, q_2, \omega) f_2(q_2, q_1, \omega), \quad (\text{A20})$$

$$f_3(q_1, q_2, \omega) = \omega \chi_{q_1, q_2}^{(1)}(\omega) + \omega_{q_2} [\omega_{q_2} \chi_{q_1, q_2}^{(2)}(\omega) + \omega_{q_1} \chi_{q_2, q_1}^{(2)}(\omega)], \quad (\text{A21})$$

$$f_2(q_1, q_2, \omega) = \omega_{q_1} + g^2 [\chi_{q_1, q_2}^{(1)}(\omega) + \omega \chi_{q_1, q_2}^{(2)}(\omega)], \quad (\text{A22})$$

$$f_1(q_1, q_2, \omega) = 2\omega \chi_{q_1, q_2}^{(1)}(\omega) + (\omega^2 - \omega_{q_1}^2 + \omega_{q_2}^2) \chi_{q_1, q_2}^{(2)}(\omega), \quad (\text{A23})$$

$$f(q_1, q_2, \omega) = \omega^2 - \omega_{q_1}^2 - \omega_{q_2}^2 - 2g^2 \omega_{q_1} \chi_{q_1, q_2}^{(1)}(\omega), \quad (\text{A24})$$

with

$$\chi_{q_1, q_2}^{(1)}(\omega) = \sum_{k\sigma} \frac{(n_{k-q_1, \sigma} - n_{k\sigma}) (\omega + \varepsilon_{k-q_1} - \varepsilon_k)}{(\omega + \varepsilon_{k-q_1} - \varepsilon_k)^2 - \omega_{q_2}^2}, \quad (\text{A25})$$

and

$$\chi_{q_1, q_2}^{(2)}(\omega) = \sum_{k\sigma} \frac{n_{k-q_1, \sigma} - n_{k\sigma}}{(\omega + \varepsilon_{k-q_1} - \varepsilon_k)^2 - \omega_{q_2}^2}. \quad (\text{A26})$$

Equation (A17) gives equation (11) of the text if we put $q_2 = -q_1$ and keep only those terms independent of g in the numerator.

Appendix B

In this appendix we give an approximate solution of equation (39). Since we are interested in the two-phonon mode whose frequency is less than $2\omega_D$ (i.e., $x < 2/r$), we can expand the logarithmic term in (36) in the form

$$\ln \left| 1 - \frac{4}{r^2 x^2} \right| \approx \frac{4}{r^2 x^2} - 2. \quad (\text{B1})$$

Using this together with (36) we can write (39) as

$$(1 - C)x^4 - [B(1 - C) + D]x^2 + (BD - 2A) = 0, \quad (\text{B2})$$

where

$$A = 432t^2 \tilde{\omega}_0^{-1} \coth(K\tilde{T})^{-1},$$

$$B = 4S \ln \tilde{T},$$

$$C = Ar^3/16,$$

$$D = \tilde{\omega}_0^{-2} - Ar/4.$$

The roots of (B2) are given by

$$x^2 = \frac{1}{2}(1 - C)^{-1} \{ [B(1 - C) + D] \pm [B(1 - C) - D] \\ \times (1 + 4A(1 - C)/[B(1 - C) - D]^2)^{1/2} \}. \quad (\text{B3})$$

Since A contains the anharmonic parameter t which is very small ($t \ll 1$) the square root in (B3) can be expanded to keep only the first term and then the roots can be written as

$$x_1^2 \approx B - 2A/[D - B(1 - C)], \quad (\text{B4a})$$

$$x_2^2 \approx D/(1 - C) + 2A/[D - B(1 - C)]. \quad (\text{B4b})$$

It can be easily checked that the first root corresponds to the two-phonon mode, the frequency of which is approximately twice that of the Kohn anomaly phonon and decreases with increasing t , and the second root corresponds to the original Raman-active phonon whose frequency increases with increasing t . Because of the expansion of (B1) we missed the root corresponding to the logarithmic singularity around $\omega = 2\omega_D$.

The dependence of the roots on the electron-phonon coupling constant s is also evident from (B4). The frequency (x_1) of the two-phonon mode, because of its dominant dependence on B , is expected to increase almost as \sqrt{s} whereas the increase of x_2 will be rather small.

Since all the quantities, A , B , C and D depend on temperature it is not easy to see the temperature dependence of x_1 and x_2 from (B4). However, for high temperatures one can use $\coth(K\tilde{T})^{-1} \approx K\tilde{T}$ and considering the values of other parameters it can be shown that the two-phonon mode frequency increases with temperature.

These qualitative features are borne out in the numerical results for the spectral function presented in figures 1–3.

References

- Balseiro C A and Falicov L M 1979 *Phys. Rev.* **B20** 4457
Behera S N and Samsur S K 1981 *J. Phys. (Paris)* **C6** 528
Berlinsky A J 1979 *Rep. Prog. Phys.* **42** 1243
Bilbro G and Mc Millan W L 1976 *Phys. Rev.* **B14** 1887
Friend R H and Jerome D 1979 *J. Phys.* **C12** 1441
Kawabata A 1971 *J. Phys. Soc. Jpn* **30** 68
Klein M V 1981 *Phys. Rev.* **B24** 4208
Klein M V 1982a in *Light scattering in solids III* (ed.) M Cardona and G Guntherodt (Berlin: Springer Verlag)
Klein M V 1982b *Phys. Rev.* **B25** 7192
Maldague P F and Tsang J C 1978 in *Proceedings Int. Conf. on Lattice Dynamics, Paris, 1977* (ed.) M. Balkanski (Paris: Flammarion) p. 602
Moncton D E, Axe J D and Di Salvo F J 1977 *Phys. Rev.* **B16** 801
Nagaosa N and Hanamura E 1982 *Solid State Commun.* **41** 809
Nagaosa N and Hanamura E 1984 *Phys. Rev.* **B29** 2060
Rietschel H 1973 *Solid State Commun.* **13** 1859
Rietschel H 1974 *Solid State Commun.* **14** 699
Smith J E, Tsang J C and Shafer M W 1976 *Solid State Commun.* **19** 283
Sooryakumar R, Klein M V and Frindt R F 1981 *Phys. Rev.* **B23** 3222
Sooryakumar R and Klein M V 1981 *Phys. Rev.* **B23** 3213
Spengler W and Kaiser R 1976 *Solid State Commun.* **18** 881
Steigmeyer E F, Harbecke G, Auderset H and Di Salvo F J 1976 *Solid State Commun.* **20** 667
Sugai S and Murase K 1982 *Phys. Rev.* **B25** 2418
Toombs G A 1978 *Phys. Rep.* **40** 182
Tsang J C, Smith J E and Shafer M W 1976 *Phys. Rev. Lett.* **37** 1407
Wilson J A, Di Salvo F J and Mahajan S 1975 *Adv. Phys.* **24** 117
Wipf H, Williams W S and Klein M V 1981 *Phys. Status Solidi* **B108** 489
Zubarev D N 1960 *Sov. Phys. Usp.* **3** 71